Dynamic behavior of cracked magnetoelectroelastic composites at different boundary conditions

Y. D. Stoynov

Citation: AIP Conf. Proc. **1487**, 256 (2012); doi: 10.1063/1.4758966
View online: http://dx.doi.org/10.1063/1.4758966
View Table of Contents: http://proceedings.aip.org/dbt/dbt.jsp?KEY=APCPCS&Volume=1487&Issue=1
Published by the American Institute of Physics.

Dynamic Behavior of Cracked Magnetoelectroelastic Composites at Different Boundary Conditions

Y. D. Stoynov

Faculty of Applied Mathematics and Informatics, Technical University of Sofia, Sofia 1000 Bulgaria.

Abstract. Magnetoelectroelastic material with a finite crack is considered. The crack is subjected to an anti-plane mechanical and in-plane electric and magnetic load. The fundamental solutions of the coupled system of the governing equations are derived in a closed form by the Radon transform. They are implemented in a non-hypersingular traction boundary integral equation method (BIEM).

A program code in Fortran, based on the BIEM, is created. Validation studies show the accuracy of the proposed scheme by comparing the results with the available data for impermeable and permeable cracks. Numerical examples display the dependence of the dynamic stress intensity factor (SIF) on the normalized frequency for different boundary conditions at the crack faces.

Keywords: Magnetoelectroelastic medium, anti – plane crack, BIEM, SIF
PACS: 02.30.Jr, 02.70.Pt, 75.50.Gg, 77.84.Lf, 77.84.Dy

INTRODUCTION

Magnetoelectroelastic materials (MEEM) are used in engineering structures, because of their electro-magneto-mechanical coupling effects. These effects exist in single-phase materials and in two-phase piezoelectric/ piezomagnetic composites. Magnetoelectric effect in the composite can be a hundred times larger than in a single-phase material at temperatures above room. In recent years, there is an increasing interest in fracture mechanics of MEEM, which are combination of piezoelectric and piezomagnetic phases. One of the basic and important issues of the fracture mechanics of the MEEM is the boundary conditions on the crack faces. For the piezoelectric materials there are two kinds of idealized boundary conditions-electrically permeable and impermeable crack [1-2]. For the MEEM there are four types of idealized boundary conditions [2].

The objective of this research is to consider the four idealized assumptions of electromagnetic boundary conditions for MEEM. These assumptions are:

i) electrically impermeable and magnetically permeable,
ii) electrically permeable and magnetically impermeable,
iii) fully impermeable,
iv) fully permeable.

STATEMENT OF THE PROBLEM

Let us consider linear MEE medium. The interactions between the mechanical, electrical and magnetic fields can be expressed by the following coupled constitutive equations [3,4]:

$$\begin{aligned} \sigma &= \mathbf{Cs} - \mathbf{eE} - \mathbf{qH}, \\ \mathbf{D} &= \mathbf{e}^t\mathbf{s} + \varepsilon\mathbf{E} + \mathbf{dH}, \\ \mathbf{B} &= \mathbf{q}^t\mathbf{s} + \mathbf{dE} + \mu\mathbf{H}, \end{aligned} \tag{1}$$

where σ, **D** and **B** are the second order stress tensor, the electric displacement vector and magnetic induction vector, respectively; **s,** **E** and **H** are the second order strain tensor, the electric field vector and the magnetic field vector, respectively; **C,** ε and μ are the fourth order elastic modulus tensor, the second order dielectric constant tensor and the magnetic permittivity tensor, respectively; **e,** **q** and **d** are piezoelectric, piezomagnetic and magnetoelectric coefficient tensors.

The MEE composite materials that we study are transversely isotropic with an axis of symmetry and poling direction along Ox_3 axis of a rectangular coordinate system $Ox_1x_2x_3$ and Ox_1x_2 is the isotropic plane. Our attention

Application of Mathematics in Technical and Natural Sciences
AIP Conf. Proc. 1487, 256-263 (2012); doi: 10.1063/1.4758966

is focused on the case when the MEEM is subjected to an external antiplane mechanical, and inplane electric and magnetic load with respect to the isotropic plane Ox_1x_2. The electric and magnetic fields are potential and the problem is two-dimensional (the material properties are the same in all planes perpendicular to the axis of symmetry). The constitutive equations in this case are [3,5]:

$$\begin{aligned} \sigma_{i3} &= c_{44}u_{3,i} + e_{15}\varphi_{,i} + q_{15}\psi_{,i} \\ D_i &= e_{15}u_{3,i} - \varepsilon_{11}\varphi_{,i} - d_{11}\psi_{,i} \\ B_i &= q_{15}u_{3,i} - d_{11}\varphi_{,i} - \mu_{11}\psi_{,i}. \end{aligned} \tag{2}$$

Here c_{44} is the elastic module, e_{15} is the piezoelectric coefficient, q_{15} is the piezomagnetic coefficient, ε_{11} is the dielectric permittivity, μ_{11} is the magnetic permeability, d_{11} is the magnetoelectric coefficient, u_3 is the out-of-plane mechanical displacement, φ and ψ are electric and magnetic potential respectively, σ_{i3} is the mechanical stress, D_i is the inplane electrical displacement, B_i is the inplane magnetic induction, $i = 1,2$ and comma means differentiation. Applying the equation of motion in the absence of body forces, the equations of Maxwell in the absence of electric charges and current densities and (2) we obtain the system of governing equations [3]:

$$\begin{aligned} c_{44}\Delta u_3 + e_{15}\Delta\varphi + q_{15}\Delta\psi &= \rho\frac{\partial^2 u_3}{\partial t^2} \\ e_{15}\Delta u_3 - \varepsilon_{11}\Delta\varphi - d_{11}\Delta\psi &= 0 \\ q_{15}\Delta u_3 - d_{11}\Delta\varphi - \mu_{11}\Delta\psi &= 0, \end{aligned} \tag{3}$$

where Δ is a two-dimensional Laplace operator and ρ is the density. In our study the MEEM is subjected to a time-harmonic external load and all field quantities are harmonic with frequency ω of the incident wave. In this case we can suppress the common factor $e^{i\omega t}$ and write the system (3) in the following way:

$$\begin{aligned} c_{44}\Delta u_3 + e_{15}\Delta\varphi + q_{15}\Delta\psi + \rho\omega^2 u_3 &= 0 \\ e_{15}\Delta u_3 - \varepsilon_{11}\Delta\varphi - d_{11}\Delta\psi &= 0 \\ q_{15}\Delta u_3 - d_{11}\Delta\varphi - \mu_{11}\Delta\psi &= 0, \end{aligned} \tag{4}$$

where u_3, φ and ψ depend only on $x = (x_1, x_2)$.

A generalized tensor of elasticity $C_{iJKl}, i,l = 1,2;\ J,K = 3,4,5$ is defined as:

$$C_{i33l} = \begin{cases} c_{44}, i = l \\ 0, i \neq l \end{cases}, C_{i34l} = C_{i43l} = \begin{cases} e_{15}, i = l \\ 0, i \neq l \end{cases}, C_{i35l} = C_{i53l} = \begin{cases} q_{15}, i = l \\ 0, i \neq l \end{cases},$$

$$C_{i44l} = \begin{cases} -\varepsilon_{11}, i = l \\ 0, i \neq l \end{cases}, C_{i45l} = C_{i54l} = \begin{cases} -d_{11}, i = l \\ 0, i \neq l \end{cases}, C_{i55l} = \begin{cases} -\mu_{11}, i = l \\ 0, i \neq l \end{cases}.$$

Using generalized displacement vector $u_J = (u_3, \varphi, \psi)$, and generalized stress tensor $\sigma_{iJ} = (\sigma_{i3}, D_i, B_i)$, $i = 1,2$, $J = 3,4,5$, the constitutive equations have the form:

$$\sigma_{iJ} = C_{iJKl}u_{K,l}.$$

Here we assume summation under repeated indexes.

The governing equations can be written in the compact form:

$$\sigma_{iJ,i} + \rho_{JK}\omega^2 u_K = 0,$$

where $\rho_{JK} = \begin{cases} \rho, J = K = 3 \\ 0, J, K = 4 \text{ or } 5 \end{cases}$. We consider the case when the crack is horizontal along Ox_1 axis and occupies the interval (-*c*,*c*), where *c*=*5mm* . The interaction of the incident wave with the crack $\Gamma = \Gamma^+ \cup \Gamma^-$, where Γ^+ is the upper bound and Γ^- is the lower bound of the crack, induces scattered waves. The total wave field at any point can be found as a superposition of the incident and scattered wave fields:

$u_J = u_J^{in} + u_J^{sc}$

and

$t_J = t_J^{in} + t_J^{sc}$.

Here u_J is the total generalized displacement, t_J is the total generalized traction defined as $t_J = \sigma_{iJ} n_i$, where $n = (n_1, n_2)$ is the normal vector to the crack, u_J^{in} and t_J^{in} are the displacement and traction of the incident wave field and u_J^{sc} and t_J^{sc} are the displacement and traction of the scattered by the crack wave field. The incident wave field is known (see [6]). The scattered field has to be determined so that the Sommerfeld's radiation condition at infinity and the boundary conditions at the crack faces are satisfied.

We will consider the following types of electromagnetic boundary conditions:

Electrically impermeable and magnetically permeable crack (type I) In this case the crack is free of mechanical tractions and surface charges, but continuity of the magnetic potential is assumed:

$t_3\Big|_\Gamma = 0$, $t_4\Big|_\Gamma = 0$, $t_5\Big|_\Gamma = B^{cr}$, $\Delta\psi = \psi^+ - \psi^- = 0$, $B^{cr} = B^+ = B^-$. Here ψ^+ and B^+ are the magnetic potential and the normal component of the magnetic induction at Γ^+, ψ^- and B^- are the magnetic potential and the normal component of the magnetic induction at Γ^- and B^{cr} is the normal component of the magnetic induction inside the crack. Therefore the boundary conditions on Γ can be written as:

$t_J^{sc} = -t_J^{in}, J = 3,4$, $t_5^{sc} = B^{cr} - t_5^{in}$.

Electrically permeable and magnetically impermeable crack (type II) The crack is free of mechanical tractions and surface currents, but continuity of the electric potential is assumed:

$t_3\Big|_\Gamma = 0$, $t_4\Big|_\Gamma = D^{cr}$, $t_5\Big|_\Gamma = 0$, $\Delta\varphi = \varphi^+ - \varphi^- = 0$, $D^{cr} = D^+ = D^-$. Here φ^+ and D^+ are the electric potential and the normal component of the electric displacement at Γ^+, φ^- and D^- are the electric potential and the normal component of the electric displacement at Γ^- and D^{cr} is the normal component of the electric displacement inside the crack. Therefore the boundary conditions on Γ can be written as:

$t_J^{sc} = -t_J^{in}, J = 3,5$, $t_4^{sc} = D^{cr} - t_4^{in}$.

Fully impermeable crack (type III) The crack faces are free of mechanical traction, surface charges and currents:

$t_3\Big|_\Gamma = 0$, $t_4\Big|_\Gamma = 0$, $t_5\Big|_\Gamma = 0$ or $t_J^{sc} = -t_J^{in}, J = 3,4,5$ on Γ.

Fully permeable crack (type IV) The crack is free of mechanical traction, but continuity of electric and magnetic potentials is assumed:

$t_3\Big|_\Gamma = 0$, $t_4\Big|_\Gamma = D^{cr}$, $t_5\Big|_\Gamma = B^{cr}$.

We will solve the respective boundary value problem for (1) transforming it into an equivalent integro – differential system of equations on the crack Γ and then solve this system numerically.

NON-HYPERSINGULAR BIEM

Following Wang and Zhang [7] for the piezoelectric case we obtain the BIE:

$$t_J^{in}(x) = -C_{iJKl}(x) n_i(x) \int_\Gamma [(\sigma^*_{\eta PK}(x,y,\omega)\Delta u_{P,\eta}(y,\omega) - \rho_{QP}\omega^2 u^*_{QK}(x,y,\omega)\Delta u_P(y,\omega))\delta_{\lambda l} - \sigma^*_{\lambda PK}(x,y,\omega)\Delta u_{P,l}(y,\omega)] n_\lambda(y) d\Gamma(y) \quad (5)$$

Here x is the observation point, $x \in \Gamma$, y is the integration variable (also called collocation point), λ_{ij} is the Kronecker symbol, u^*_{QK} is the fundamental solution, $\sigma^*_{iPK} = C_{iPMl} u^*_{MK,l}$, t_J^{in} is the incident plane wave and $\Delta u_J = u_J\Big|_{\Gamma^+} - u_J\Big|_{\Gamma^-}$ are the unknown crack opening displacements (COD). The fundamental solution and the incident plane wave can be found in [6]. We reduce the BIE (5) to a system of linear equations and solve it numerically. The traction field in every point $x \notin \Gamma$ can be found by the corresponding representation formula (see

[6]). The stress concentration near crack tips is computed using the formula: $K_{III} = \lim_{x_1 \to \pm c} t_3 \sqrt{2\pi(x_1 \mp c)}$, where c is the half-length of the crack.

NUMERICAL REALIZATION

The numerical solution scheme follows the procedure developed in Rangelov et al. [8] A FORTRAN program is created and the numerical results are obtained using PC – Core 2 Duo CPU E8500, 3.16GHz and 2.53GHz, 3GB RAM. The MEE material that we used is piezoelectric/piezomagnetic composite $BaTiO_3/CoFe_2O_4$. The material constants of the used materials can be found in [6].

Validation Studies

We validated our numerical tool with the results of Zhou and Wang (2005) [9] for a fully permeable crack. The crack is divided into 7 and 15 boundary elements (BE). The results obtained with a mesh of 7 and 15 BE are compared with those of Zhou and Wang. The comparison is given in Fig.1. We see good coincidence of the results.

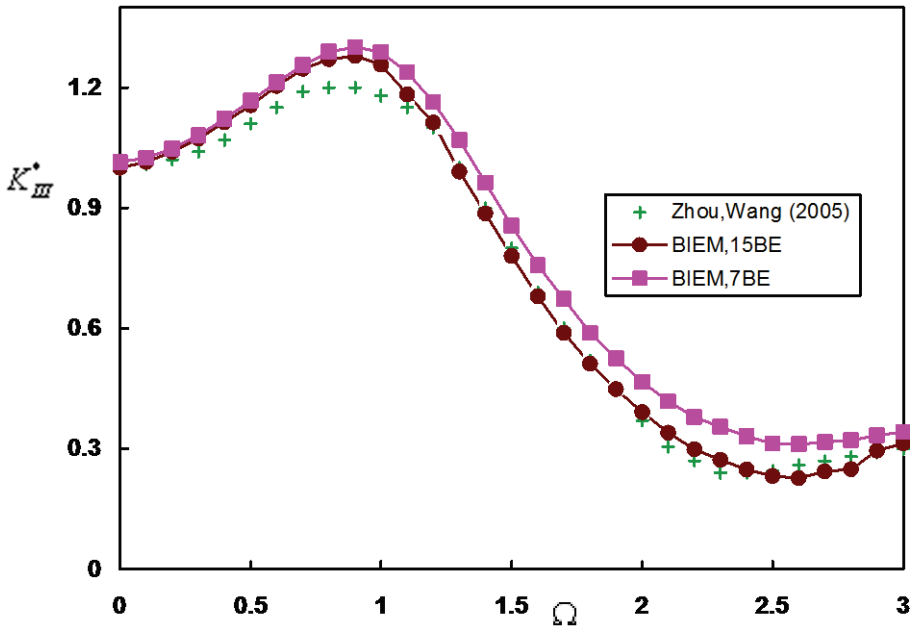

FIGURE 1. The normalized SIF $K^*_{III} = \dfrac{K_{III}}{t_3^{in}\sqrt{\pi c}}$ versus the normalized frequency $\Omega = c\sqrt{\rho \tilde{a}^{-1}}\omega$ for composite material, where $\tilde{a} = \tilde{c}_{44} + \dfrac{\tilde{e}_{15}^2}{\tilde{\varepsilon}_{11}}$, $\tilde{c}_{44} = c_{44} + \dfrac{(q_{15})^2}{\mu_{11}}$, $\tilde{e}_{15} = e_{15} - \dfrac{d_{11}q_{15}}{\mu_{11}}$, $\tilde{\varepsilon}_{11} = \varepsilon_{11} - \dfrac{(d_{11})^2}{\mu_{11}}$.

Another test with the results for piezoelectric material of Wang and Mequid [10] and Ma *et al.* [11] is presented in Figure 2. The crack is fully impermeable. We see very close coincidence of the results.

A test with the results of Rangelov *et al* [1] for the piezoelectric material $BaTiO_3$ is also shown. The crack is fully permeable. The test is given in Figure 3.

Parametric Studies

The aim of parametric studies is to show the sensitivity of the SIF to the type of the material and the type of the external load for different electromagnetic boundary conditions on the crack.

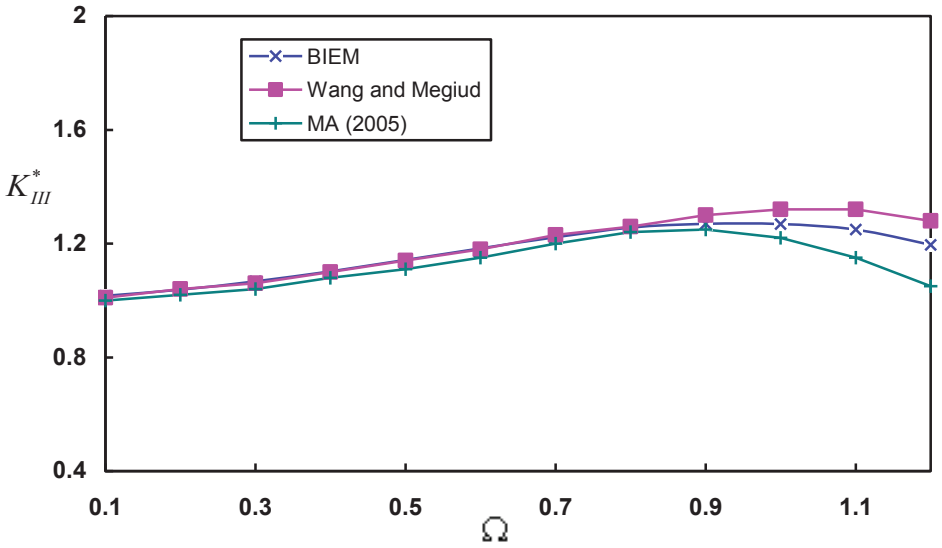

FIGURE 2. The normalized SIF versus the normalized frequency for piezoelectric material, an impermeable crack. The normalized frequency is $\Omega = c\sqrt{\rho a^{-1}}\,\omega$, where $a = c_{44} + \frac{e_{15}^2}{\varepsilon_{11}}$

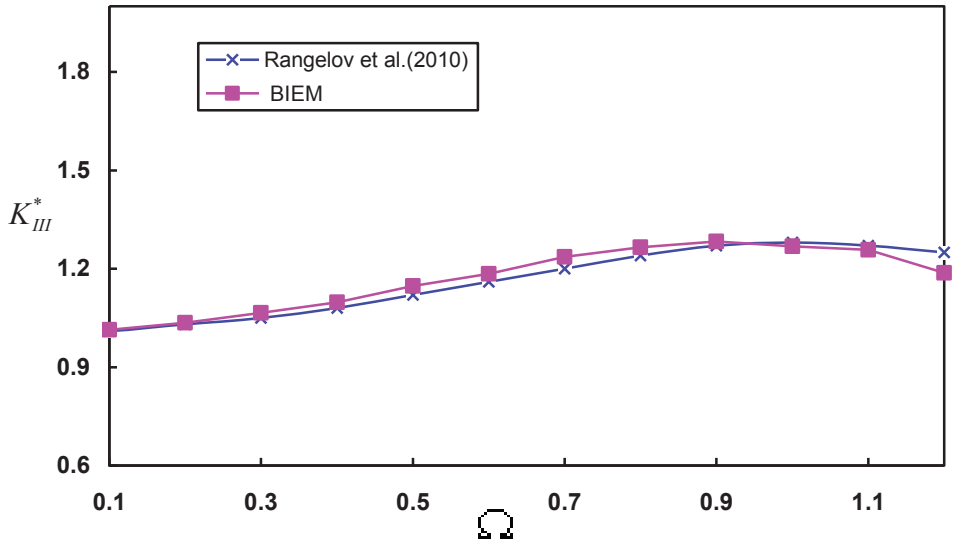

FIGURE 3. The normalized SIF versus the normalized frequency for the piezoelectric material $BaTiO_3$. The normalized frequency is $\Omega = c\sqrt{\rho c_{44}^{-1}}\,\omega$

In Fig.ure 4 the normalized SIF is plotted versus the normalized frequency for piezoelectric material $BaTiO_3$, piezomagnetic material $CoFe_2O_4$ and composite. The crack is fully permeable. The external load is an incident plane wave. The maximum value is achieved at $\Omega \approx 1.0$. The graphics show sensitivity of the SIF to the type of the material.

A comparison of a fully permeable and fully impermeable crack is given in Figure 5. MEE composite is subjected to the electromechanical external load: $t_3^{in} = \tau, t_4^{in} = D\frac{\varepsilon_{11}}{e_{15}}\tau, t_5^{in} = 0$. The comparison shows that SIFs obtained for

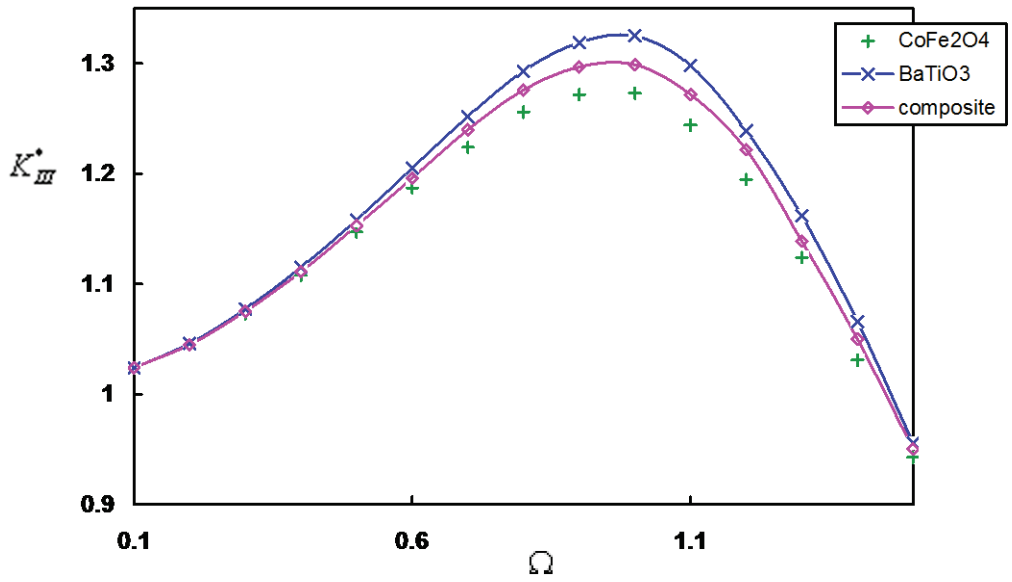

FIGURE 4. Normalized SIF versus the normalized frequency for three different materials

permeable cracks do not depend on the amplitude of the applied electrical load. The SIFs obtained for impermeable cracks depend significantly on the amplitude of the applied electrical load.

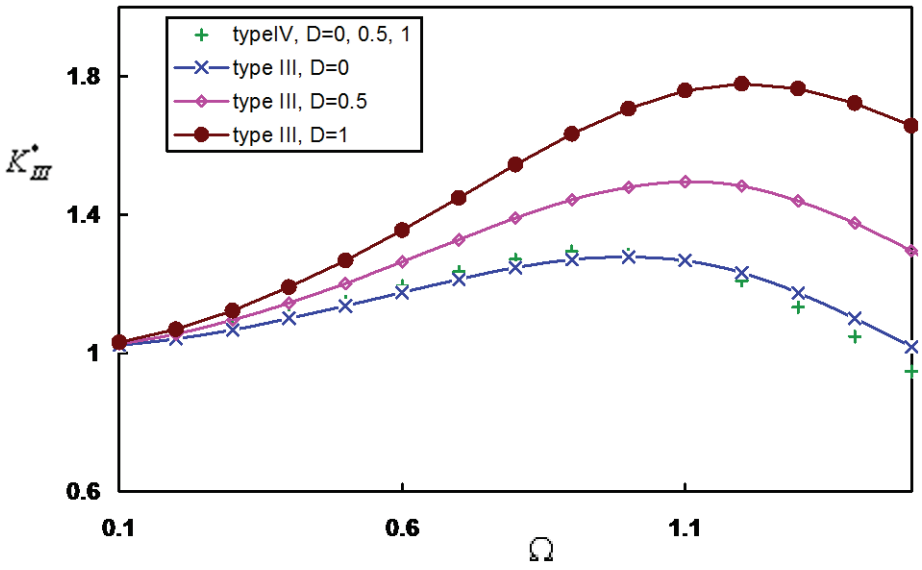

FIGURE 5. Normalized SIF versus the normalized frequency for MEEM under electromechanical load. Fully permeable and fully impermeable crack

In Figure 6 MEE composite is subjected to magnetomechanical external load: $t_3^{in} = \tau, t_4^{in} = 0, t_5^{in} = B\frac{\mu_{11}}{q_{15}}\tau$. Type II and type III cracks are compared. The SIFs obtained for both types of cracks depend significantly on the amplitude of the applied magnetic load. The results show sensitivity of the SIFs to the type of the electromagnetic boundary conditions.

In Figure 7 MEE composite is subjected to electromechanical external load: $t_3^{in} = \tau, t_4^{in} = D\frac{\varepsilon_{11}}{e_{15}}\tau, t_5^{in} = 0$. Type I and type III cracks are compared. The results show sensitivity of the SIFs to the amplitude of the applied electrical load for type I and type III cracks.

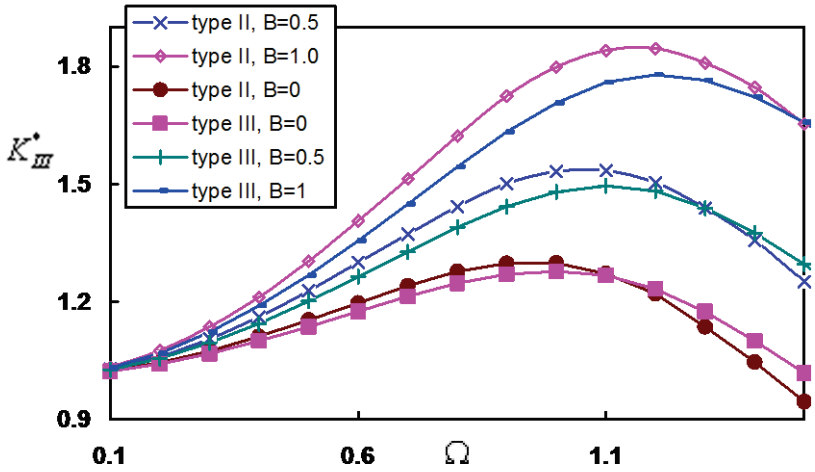

FIGURE 6. Normalized SIF versus the normalized frequency for MEEM under magnitomechanical load. Type II and type III cracks

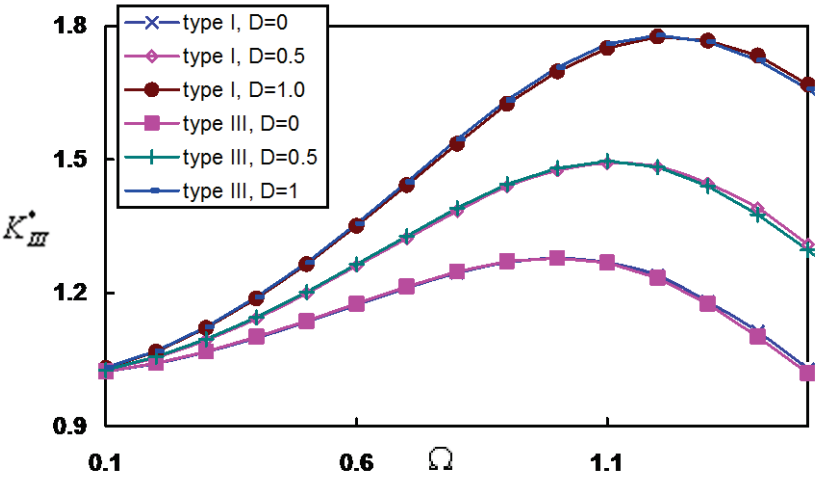

FIGURE 7. Normalized SIF versus the normalized frequency for MEEM under electromechanical load. Type I and type III cracks

In Figure 8 MEE composite is subjected to an incident plane wave. The four different types of electromagnetic boundary conditions are compared. The comparison shows close results for type I and type III cracks and also for type II and type IV cracks. It also shows that the SIFs are more sensitive to the electrical permeability than the magnetic permeability of the crack.

CONCLUSIONS

The present work is focused on the boundary conditions for MEEM with antiplane cracks. As a solution method the BIEM is used. The parametric studies reveal the significant differences that may occur when using different boundary conditions.

Here we performed a pure theoretical analysis for the MEEM with cracks. As B. Wang and J. Han mentioned, it is possible to use the present results to determine the type of the crack boundary conditions via appropriate

experiments. The present software can be developed further and results for MEEM with more than one crack under static and dynamic loads can also be obtained.

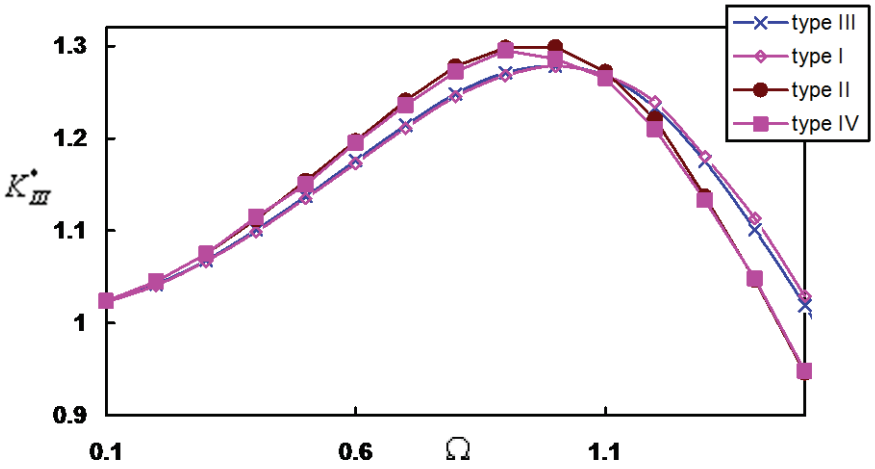

FIGURE 8. Normalized SIF versus the normalized frequency for MEEM under an incident plane wave. The four different types of crack are compared

ACKNOWLEDGMENTS

The author acknowledges the support of BNSF under the grant DID 02/15.

REFERENCES

1. T. Rangelov, P. Dineva, and D. Gross (2010) *Arch Appl Mech*, **80**, 985–996.
2. B. Wang, and J. Han (2006), *Acta Mech Sinica* **22**, 233-242.
3. X. F. Li (2005) *IJSS,* **42**, 3185–3205.
4. J. Lee, J. G. Boyd IV, and D. C. Lagoudas (2005) *International Journal of Engineering Science* **43**, 790-825.
5. L. Ma., J. Li, R. Adbelmoula, and L. Z. Wu (2007) *Int. J. Solids Str.*, 44, 5518-5537.
6. Y. Stoynov, T. Rangelov (2009) *Journal of Theoretical and Applied Mechanics* **39** 73–92.
7 C. Y. Wang, and C. Zhang (2005) *Eng. Anal. Bound. Elem.* **29**, 454–465.
8. T. Rangelov, P. Dineva, and D. Gross (2008) *ZAMM · Z. Angew. Math. Mech.* **88**, 86 – 99.
9. Z. G. Zhou, and B. Wang (2005) *Applied Mathematics and Mechanics* **26**, 17-26.
10. X. D. Wang, and S.A. Meguid (2000) *Acta Mechanica* **143**, 1-15.
11. L. Ma, L. Z. Wu, Z. G. Zhou, and L. C. Guo (2005) *Composite Structures* **69**,. 436–441.